

Actinic detection & signal characterization of multilayer defects on EUV mask blanks

Yoshihiro Tezuka^{a*}, Tsuneo Terasawa^a,
Toshihiko Tanaka^a, Toshihisa Tomie^b

^aMIRAI-ASET, Tsukuba, Japan

^bMIRAI-ASRC, AIST, Tsukuba, Japan

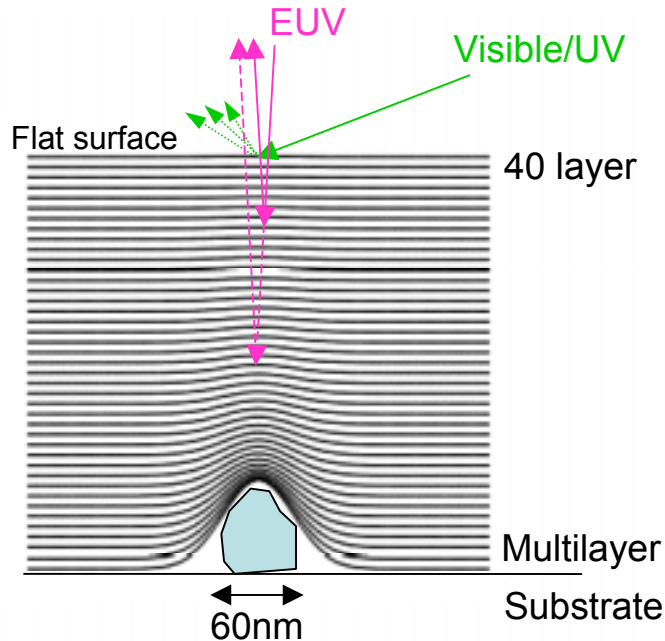
*Email: tezukay@mirai.aist.go.jp

Outline

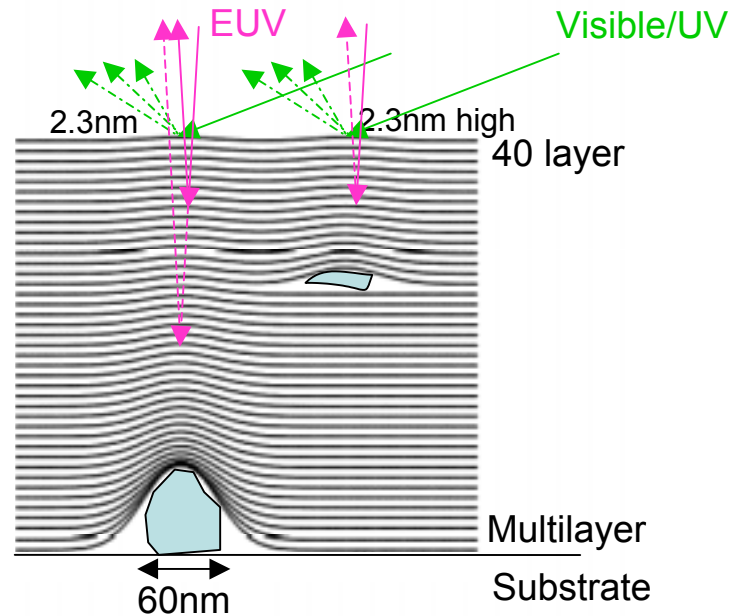
- Introduction
 - Motivation, concept, goal & scope
 - Inspection tool
 - Signal modeling
- Experimental
 - Programmed defect mask blank
 - EUV image
- Signal intensity analysis
 - Comparison with AFM
 - Detection algorithm
- Natural defect detection
 - “Critical” & “sub-critical” defect detection
- Throughput estimate
 - Noise analysis
 - EUV energy measurement
- Summary

Motivation: -potential needs-

Printable “line” defect w/ flat surface



Nuisance defects w/ same bump

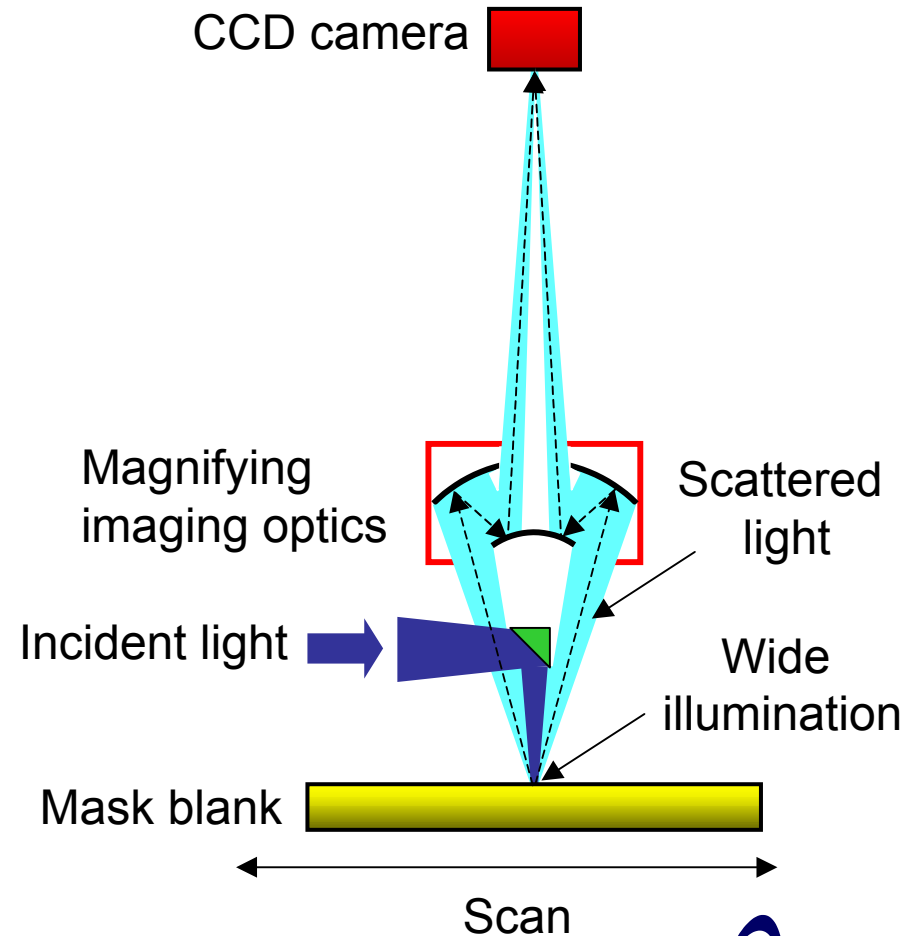


Visible/UV inspection may not be sufficient to detect all critical defects with tolerable number of nuisance defects

Concept of actinic inspection tool

- At- λ inspection for:
 - better correlation with printability
 - possible detection of “actinic-only” defects
- High speed inspection by:
 - wide illumination
 - dark-field imaging
 - CCD camera

Aimed at 2 hrs / blank



Positioning of research in MIRAI

- Goals

- Phase 1 (~FY'03)

- Demonstration of POC: Successfully Completed!

- Phase 2.1 (~FY'05)

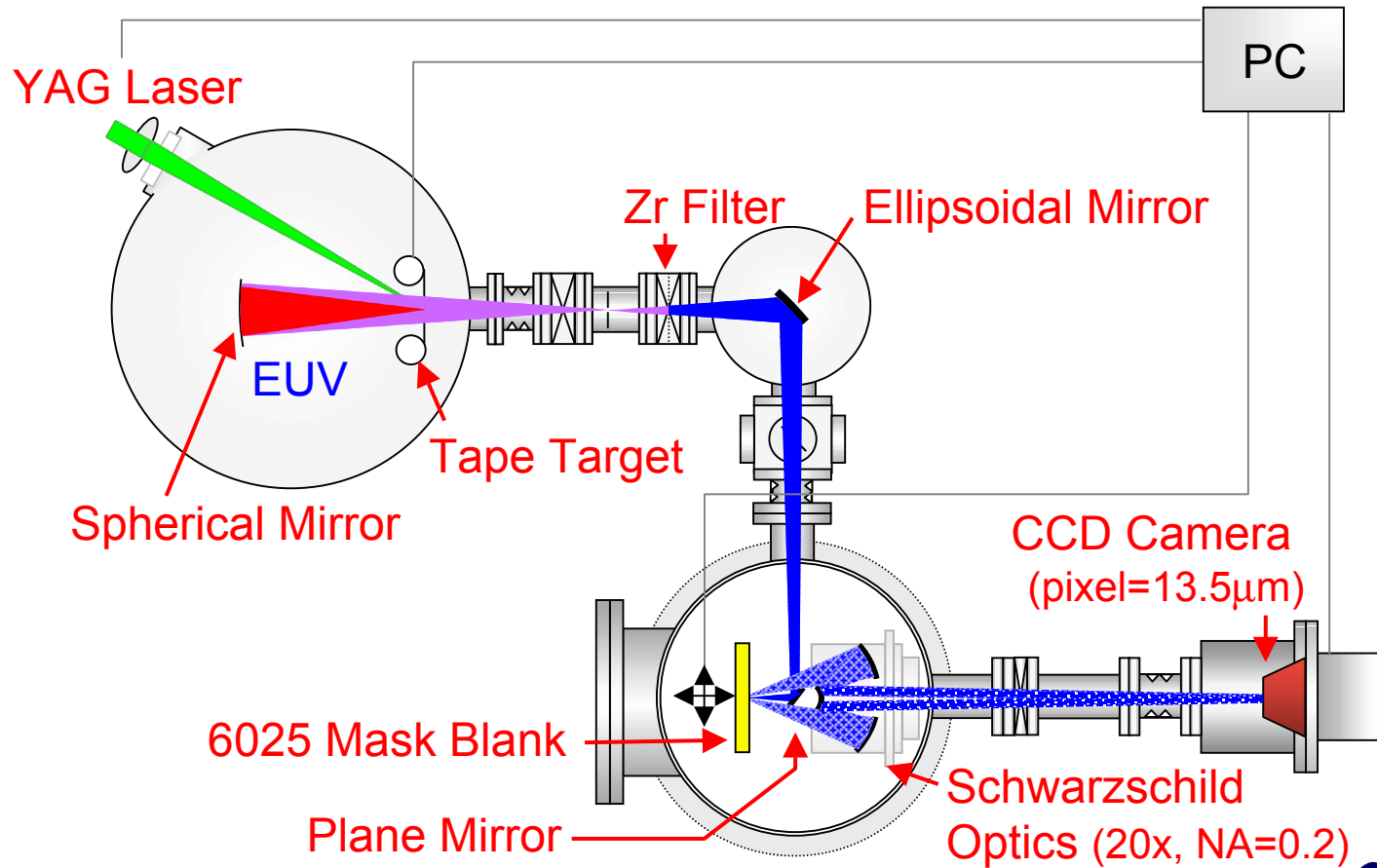
- Design completion of manufacturing-ready prototype with accumulated experimental data

- Scope

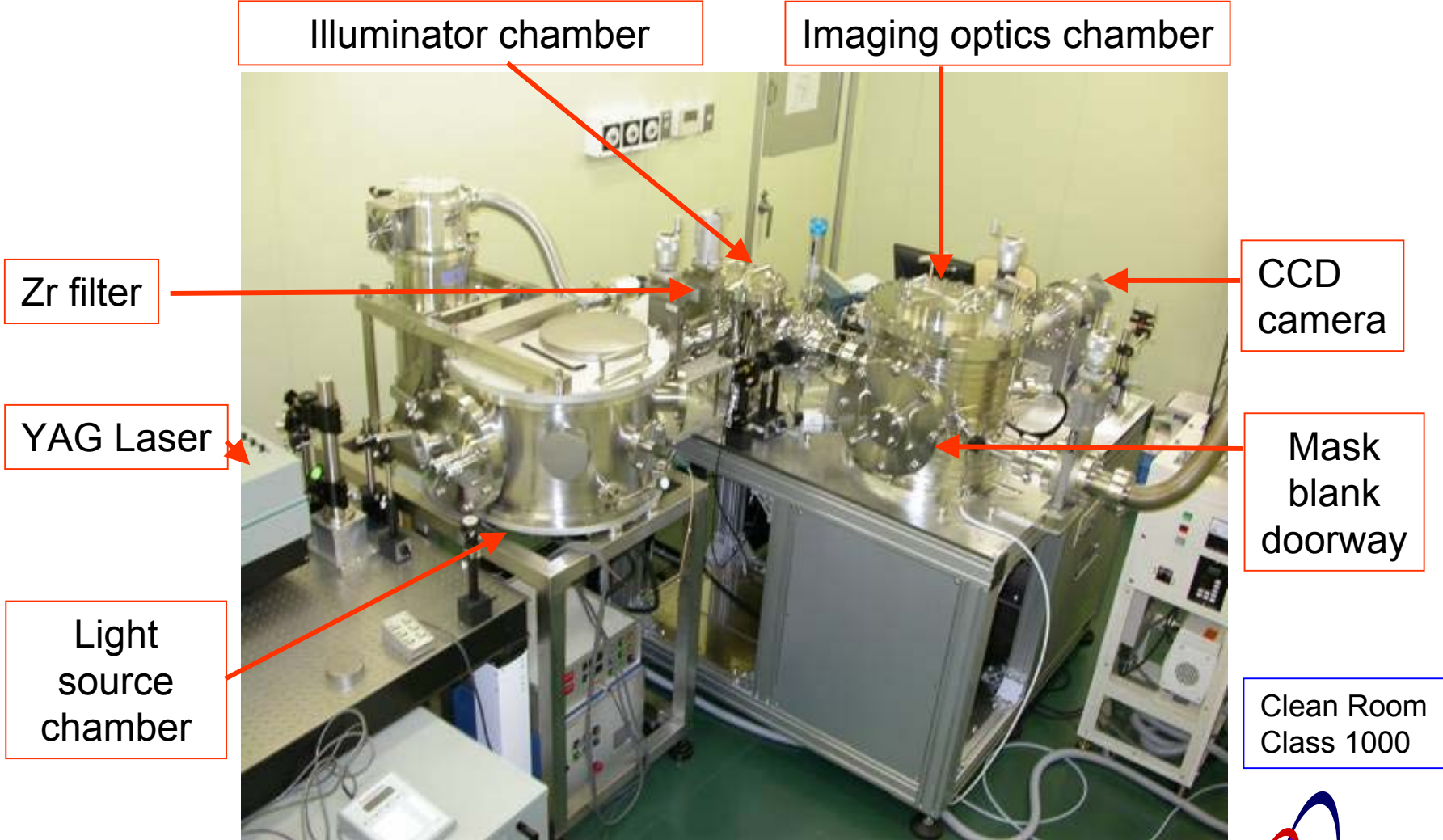
- Development of advanced yet affordable actinic mask blank inspection tool for:

- Benchmarking with non-actinic tools
 - Multilayer process development support
 - Outgoing / incoming qualification of premium mask blanks

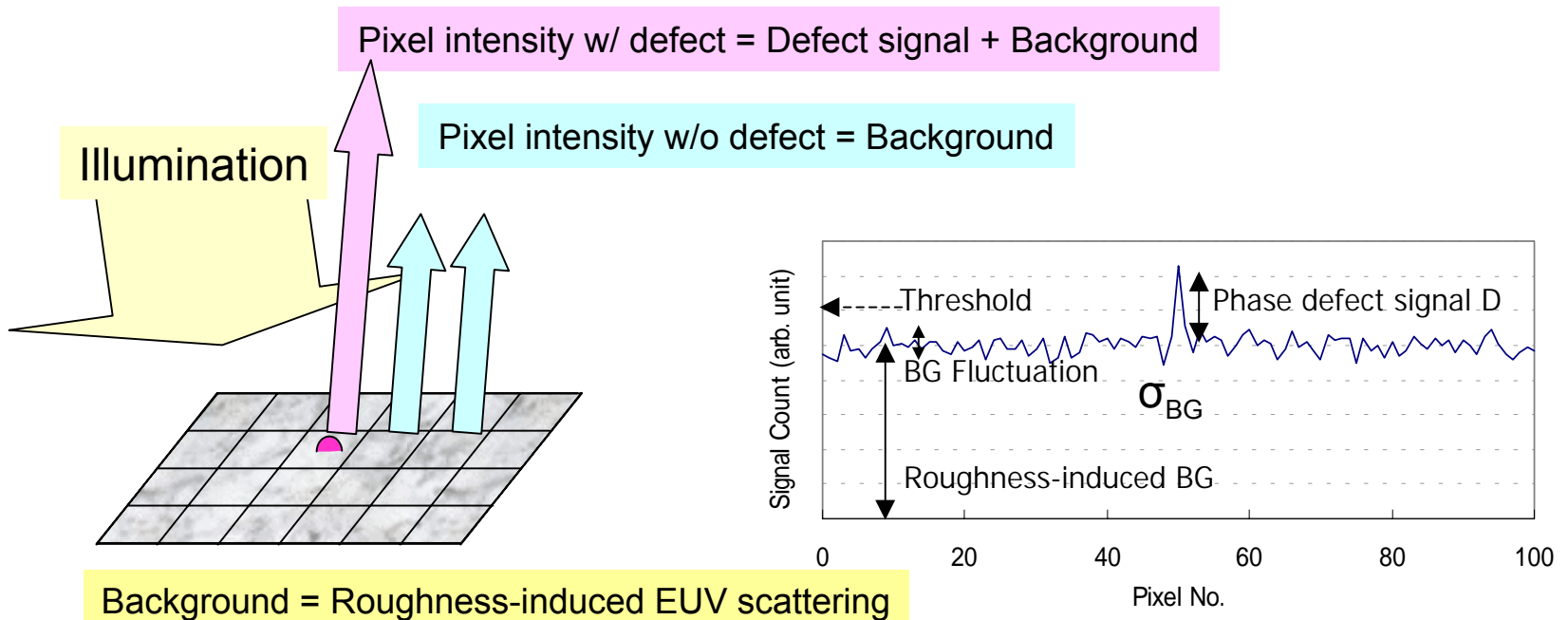
Experimental Setup



Inspection tool in MIRAI Lab



Signal modeling



Background = Roughness-induced EUV scattering

Background fluctuation $\sigma_{BG}^2 = \text{Spatial fluctuation of roughness } \sigma_{SP}^2 + \text{Shot noise } \sigma_{SH}^2$

Signal modeling procedure

- Defect signal, background: Computed by EUV diffraction/scattering
- Spatial fluctuation of roughness: Computed by random fractal
- Total noise: Computed with counting statistics of detectable photon

Signal to background ratio

- Signal intensity
 - Numerical angular integration of scattered EUV from Gaussian-shaped phase defect.

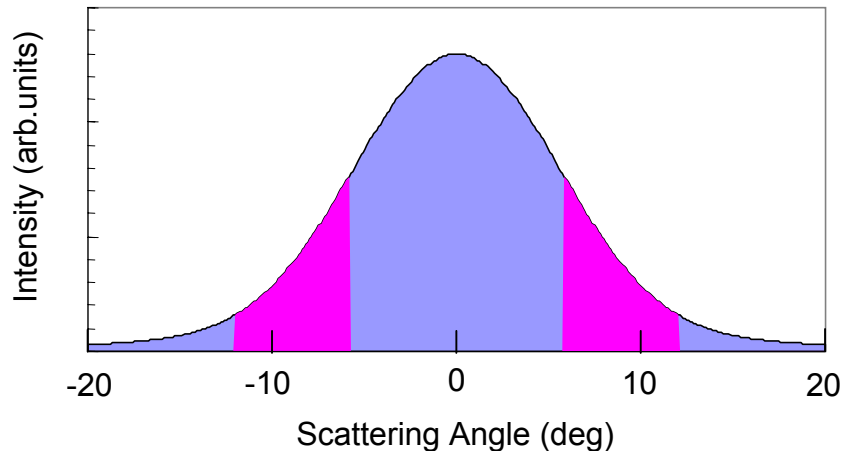


Fig. Angular distribution of scattered EUV from a 30nm (FWHM) Gaussian-shaped phase defect and integration range in MIRAI POC optics setup

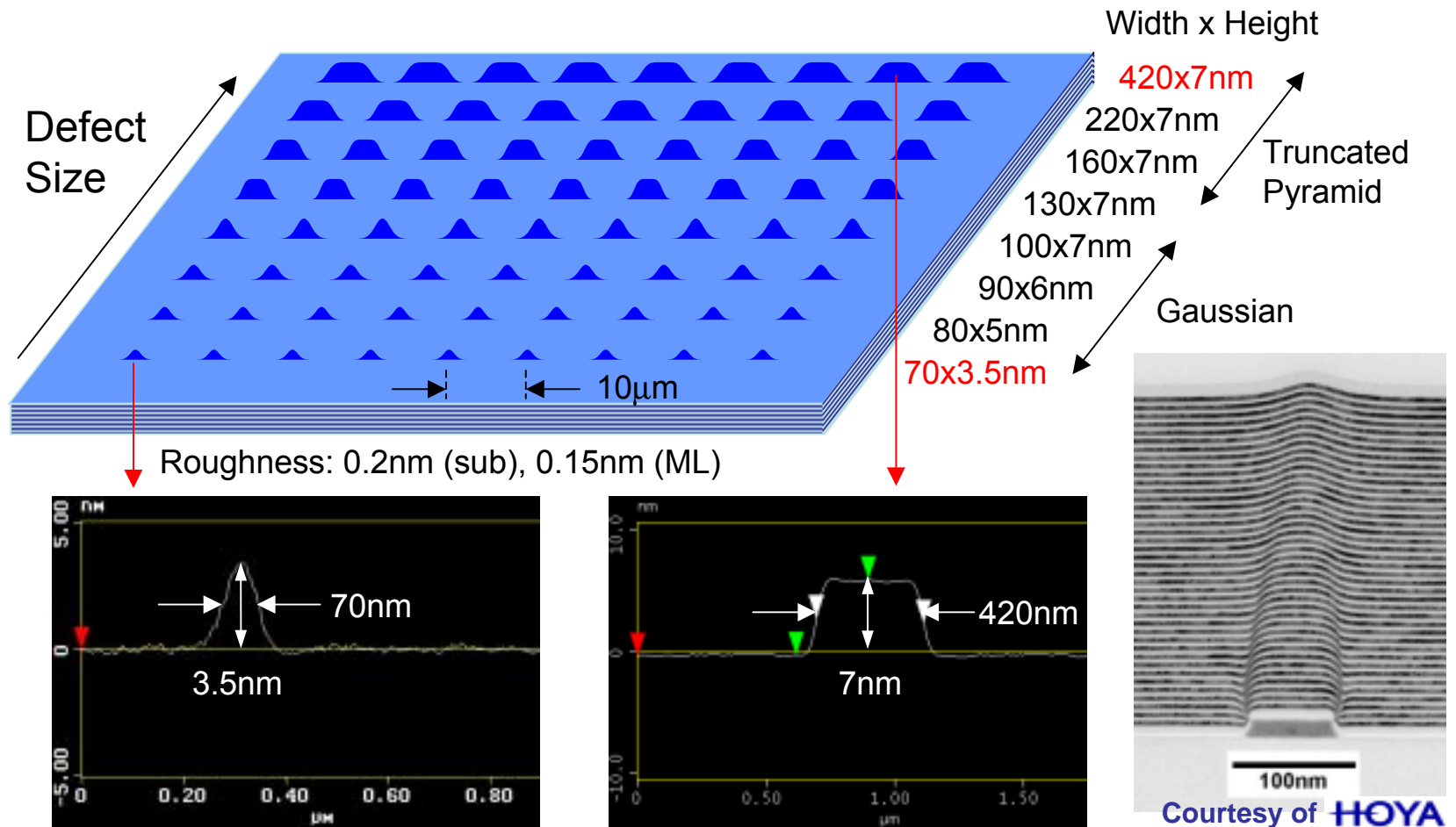
- Background intensity
 - Analytical integration assuming RMS=0.15nm with “extreme fractal” PSD(f)

$$BG = R \cdot \left(\frac{4\pi\sigma_{spec}}{\lambda} \right)^2 \cdot \frac{\int_{f_{min}}^{f_{max}} 2\pi f \cdot PSD(f) df}{\int_{F_{min}}^{F_{max}} 2\pi f \cdot PSD(f) df}$$

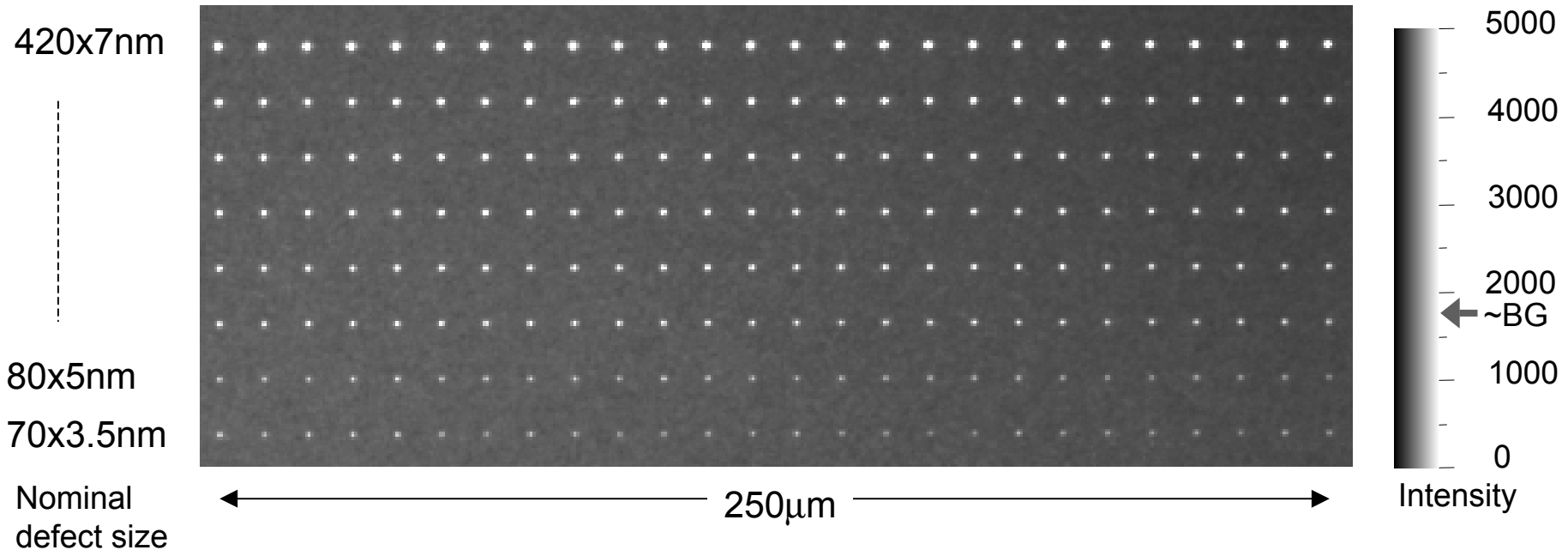
- ->BG ~ 0.12% of incident light

$$\frac{\text{Signal (30nm}^W \times \text{3nm}^H)}{\text{Background(0.675}\mu\text{m)}} = 1.3$$

Array of programmed defects



First EUV image of defect array

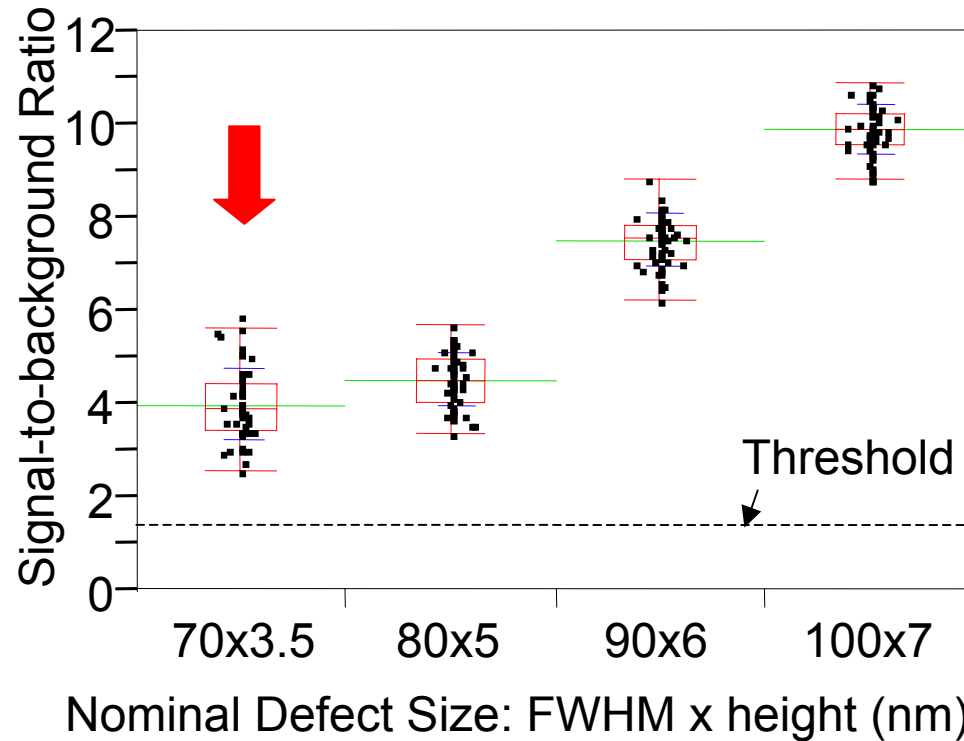


All programmed defects detected.

Calculate $\sum_{i,j}^{5 \times 5} \frac{A_{i,j} - \langle BG \rangle_{\text{Local}}}{\langle BG \rangle_{\text{Local}}}$ for each defect

$A_{i,j}$: pixel intensity

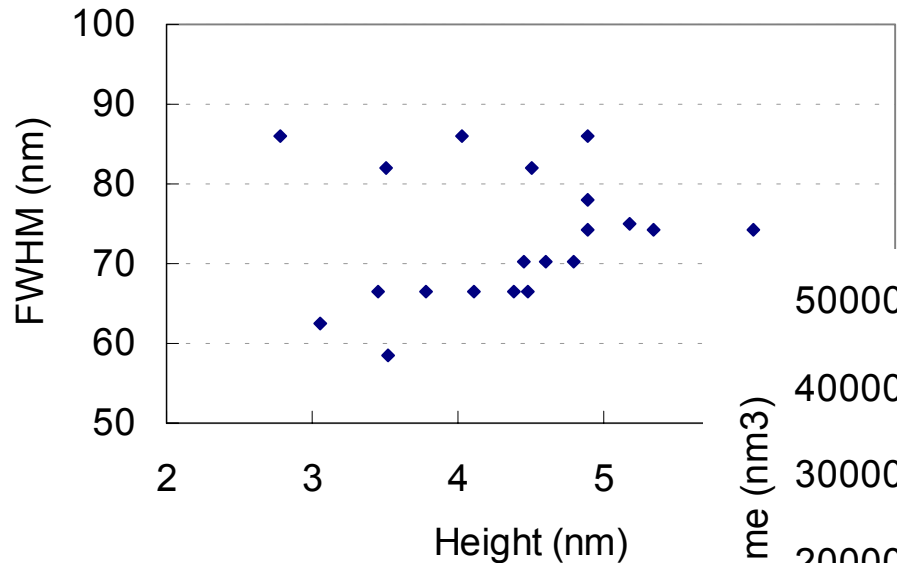
Integrated signal and screening



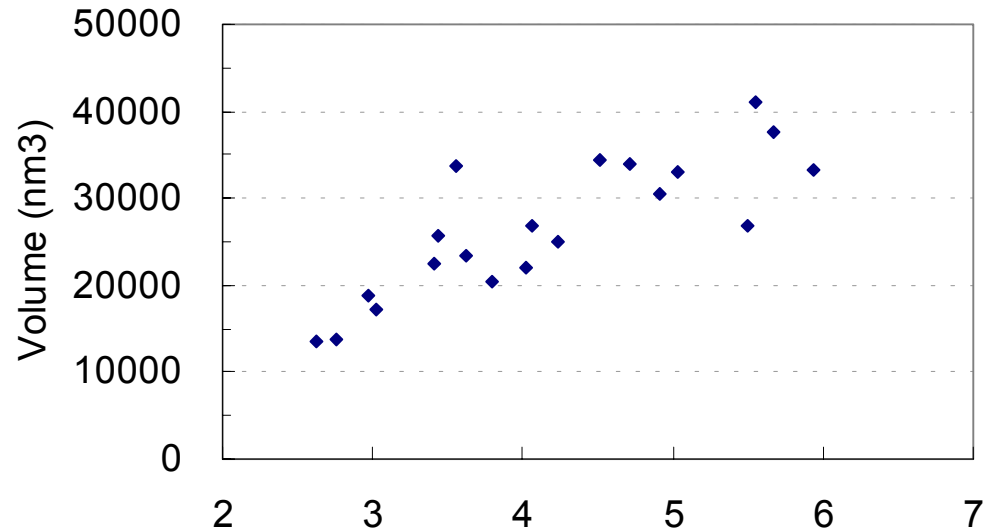
Large variation of intensity still exists

Actual size of bumps assessed by AFM

Signal correlation with bump dimension



Bump size varies
59~86nm in FWHM
2.8~6.0nm in height



Good correlation b/w signal intensity and bump volume

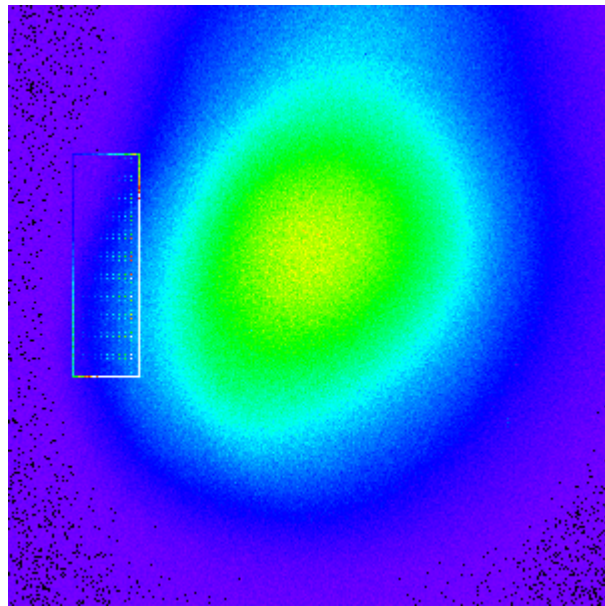
SBR variation reflects actual size variation

SBR is good metric for defect size prediction

Signal Intensity (SBR)
(SBR: signal-to-background ratio)

Illumination uniformity

- Large non-uniformity
- Temporally unstable



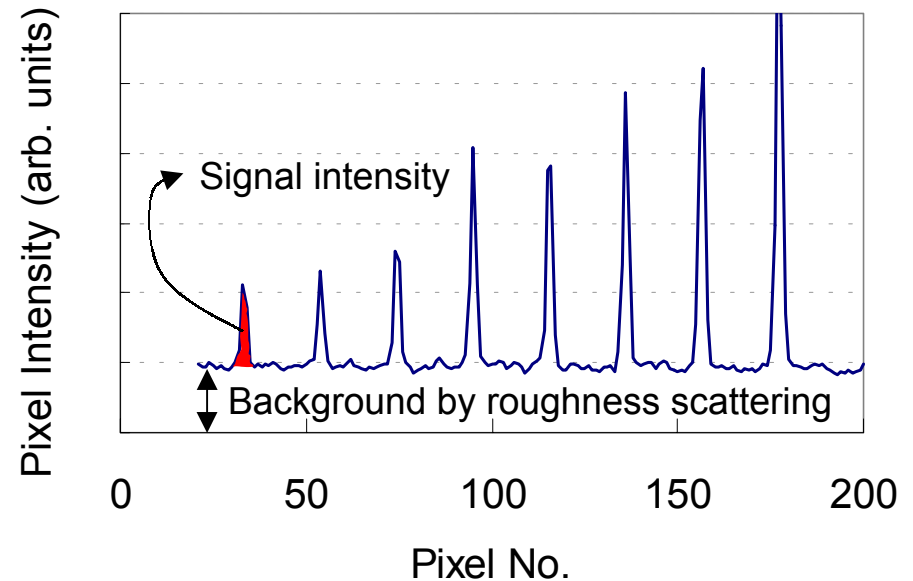
← 1.4mm →

Illumination intensity map

- SBR positively use BG, or roughness scattering

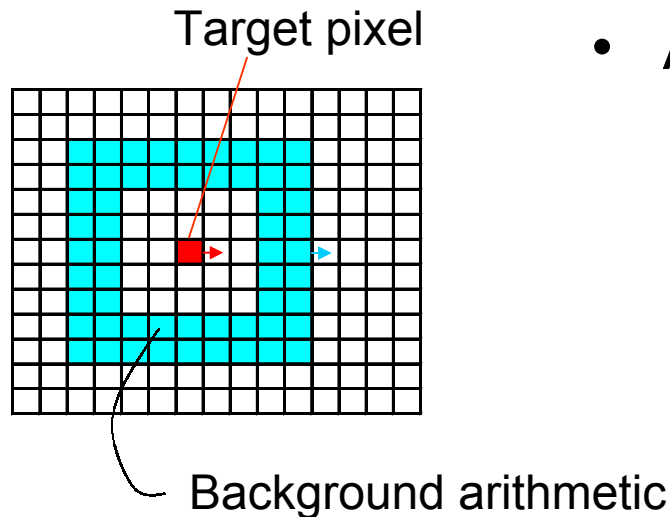
$$- \text{SBR} = \sum_{i,j} \frac{A_{i,j} - \langle \text{BG} \rangle_{\text{Local}}}{\langle \text{BG} \rangle_{\text{Local}}}$$

- Illumination-invariant



Detection algorithm

1. Normalize by local background intensity

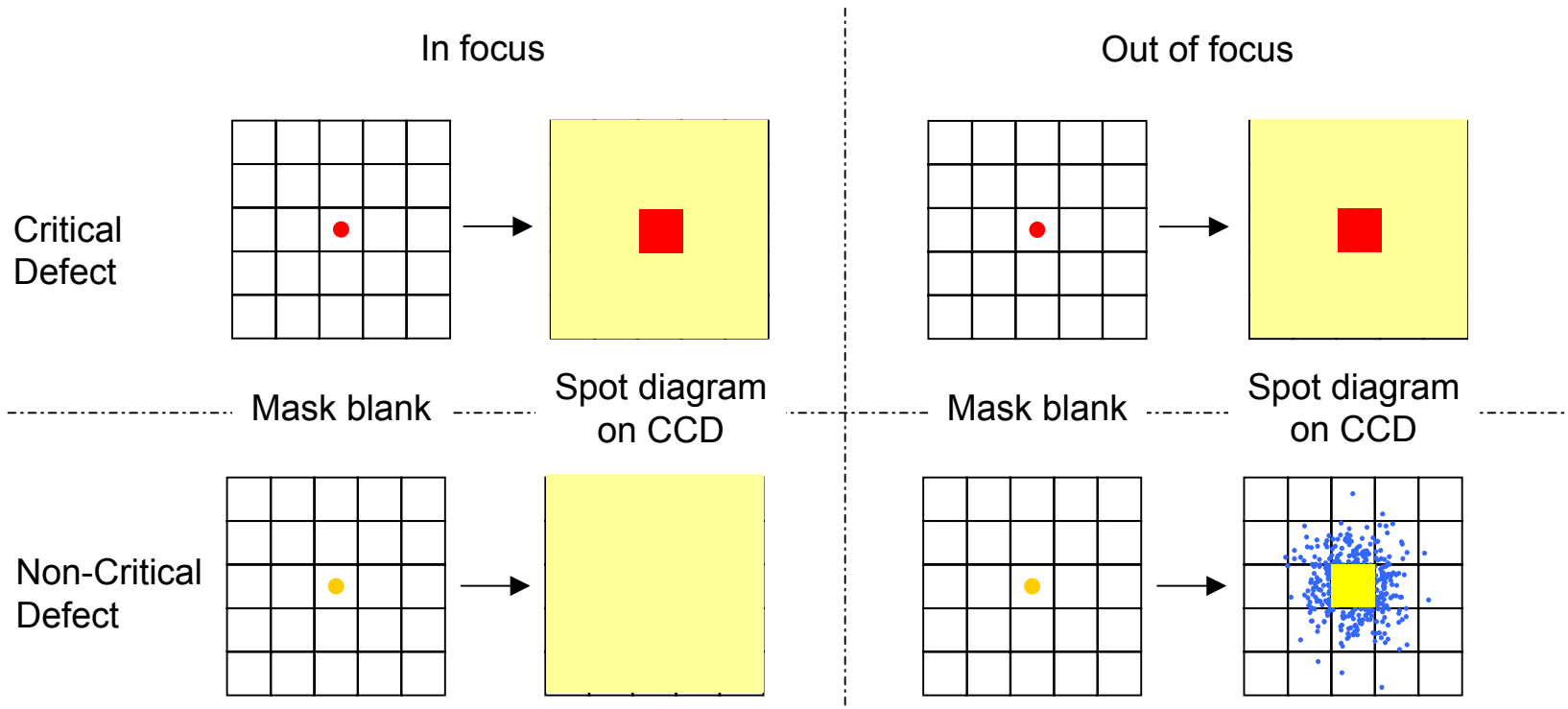


- Advantages

- Accommodate unpredictable fluctuation of illumination intensity distribution
- Good for real-time calculation with sequential data

2. Flag by statistical significance of pixel intensity
3. Screen by printability threshold using SBR
4. Store coordinates as defect

Challenge in large field of view

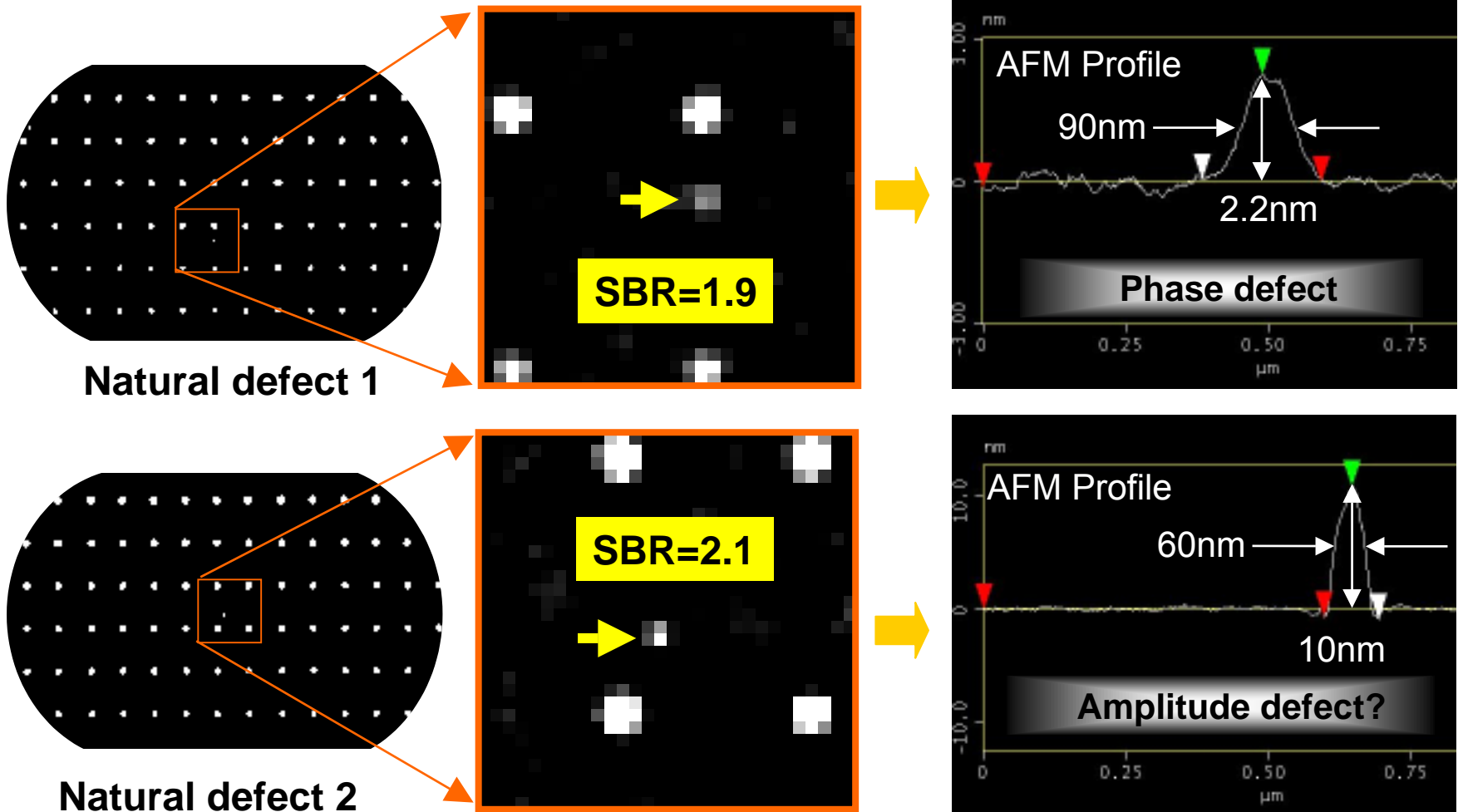


This step can accommodate aberration and field curvature of Schwarzschild optics.



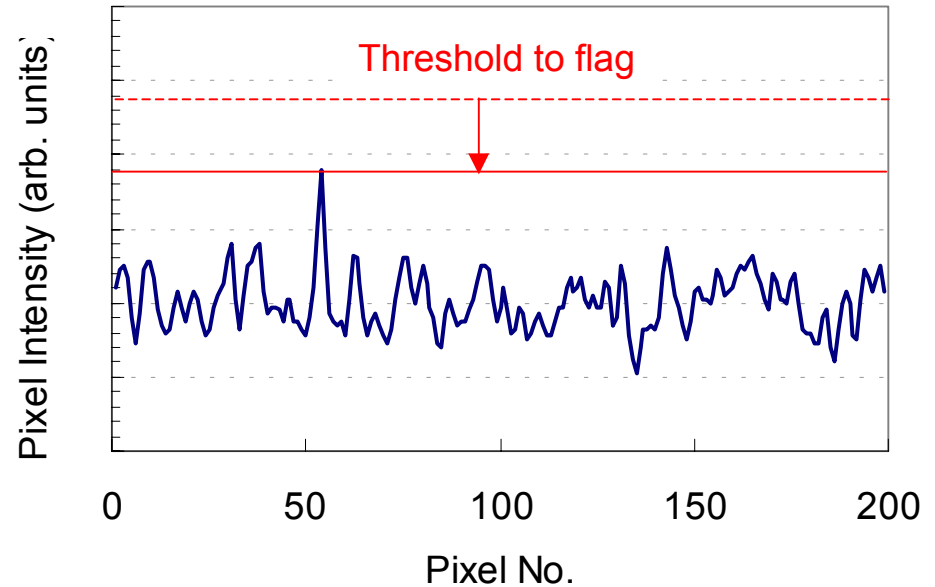
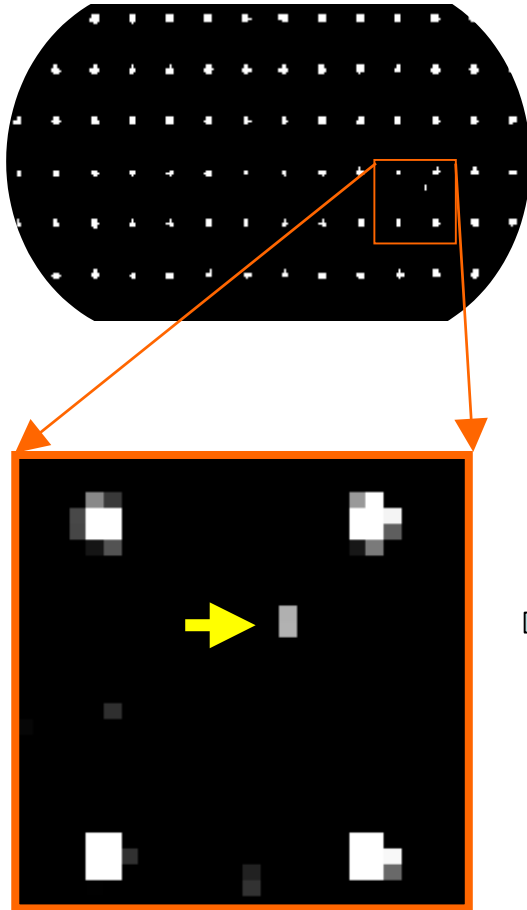
Enable to live with inexpensive spherical mirrors for imaging

Natural defects



“Sub-critical” natural defect

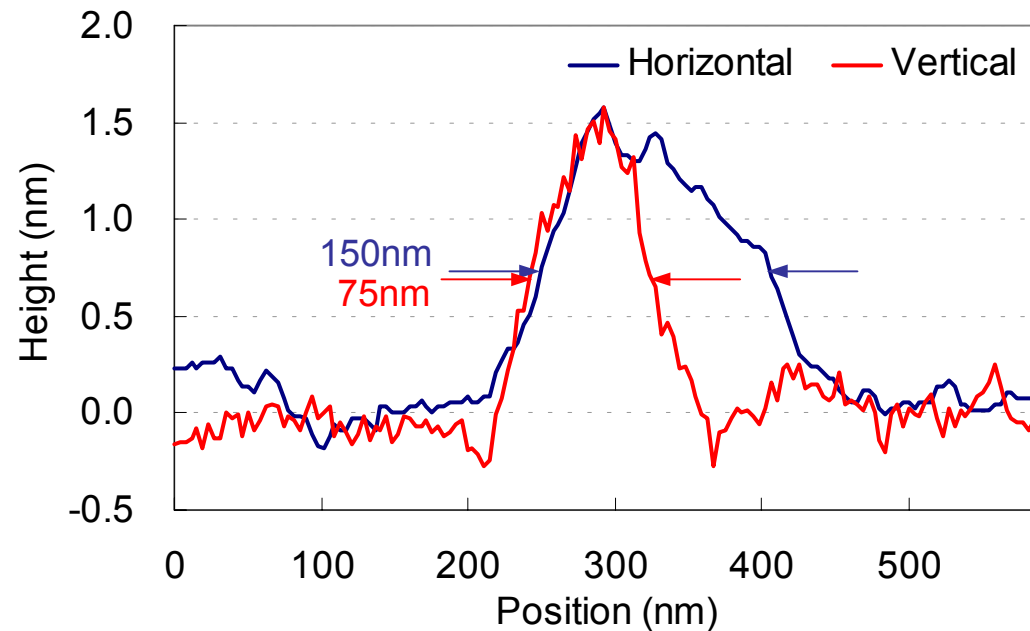
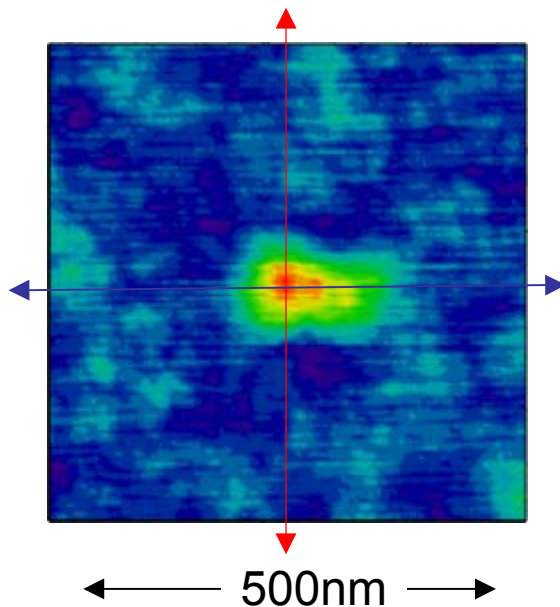
EUV Darkfield Image



SBR=1.1 < 1.3 (=Screening threshold)

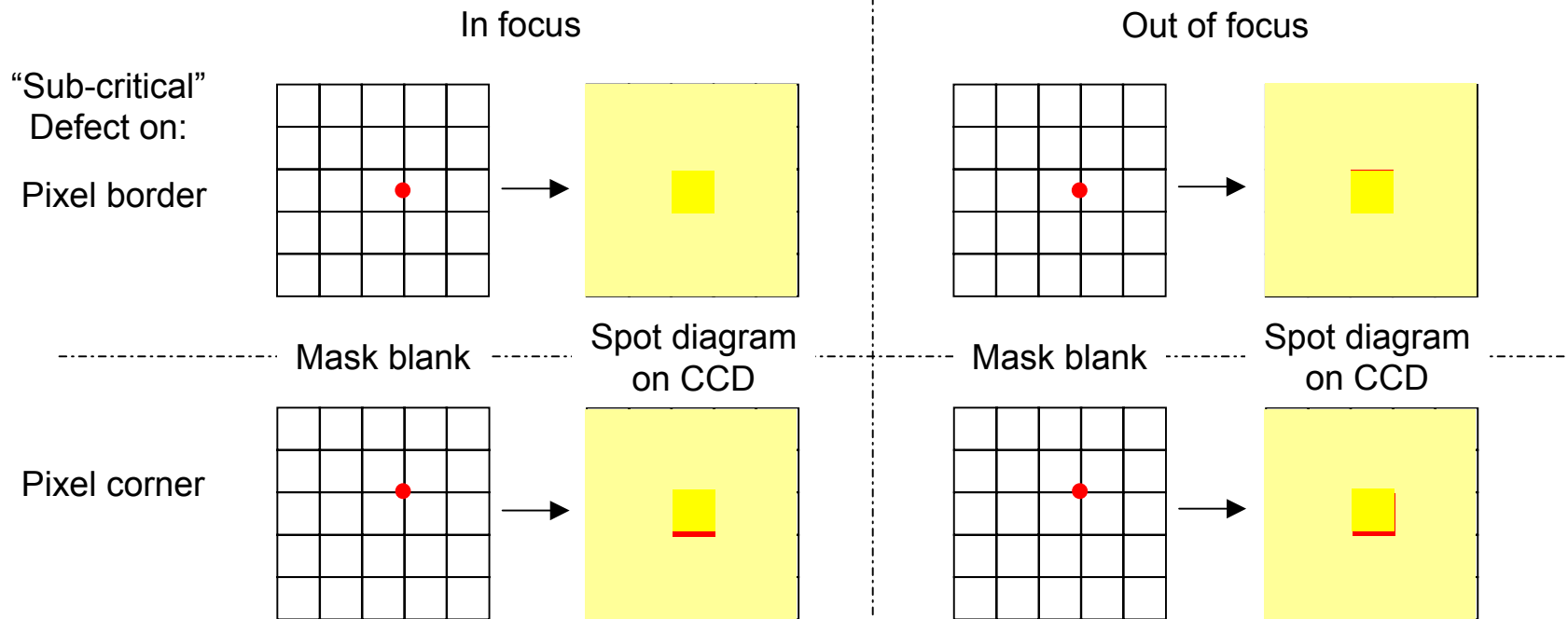
Non-printable? Location assessed by AFM

“Sub-critical” natural defect



1.5nm-high “sub-critical” natural defect “found” with a false defect estimate of ~150 in the whole area of a blank due to spatial variation of roughness.

Defect detection improvements



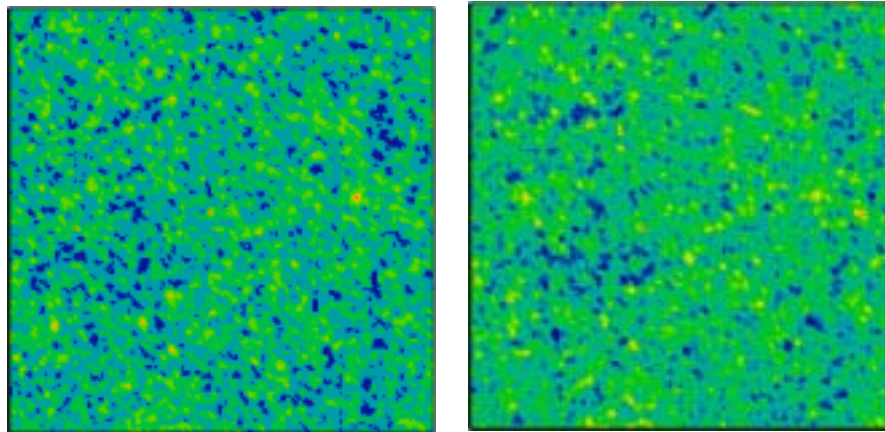
False defect count estimate reduced to ~20

Being burned into FPGA for real-time process to meet 2 hrs/blank

Detecting down to 1.5nm-high defects w/ **no** false defects will need higher magnification, ... at the expense of TPT.

Noise Analysis – repeatability -

Background Intensity Map
(128x128 pixels: 100 pulses)



1st image

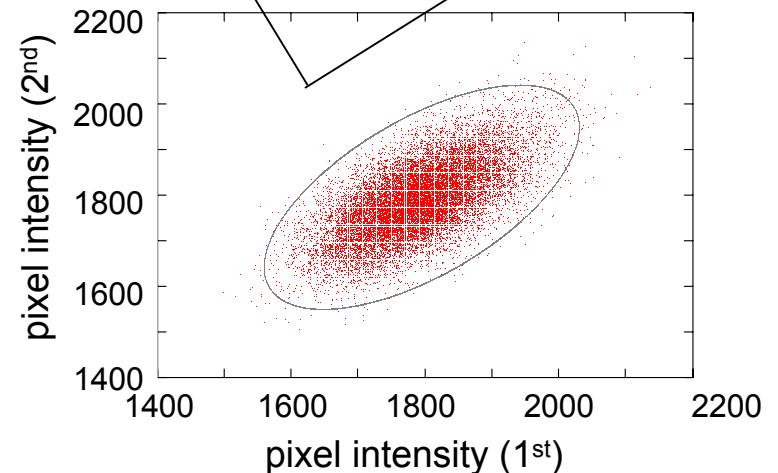
2nd image

$$\frac{\text{Shot noise } (\sigma)}{\text{mean}} = 2.6\%$$

$$\frac{\text{Roughness fluctuation } (\sigma)}{\text{mean}} = 3.5\%$$

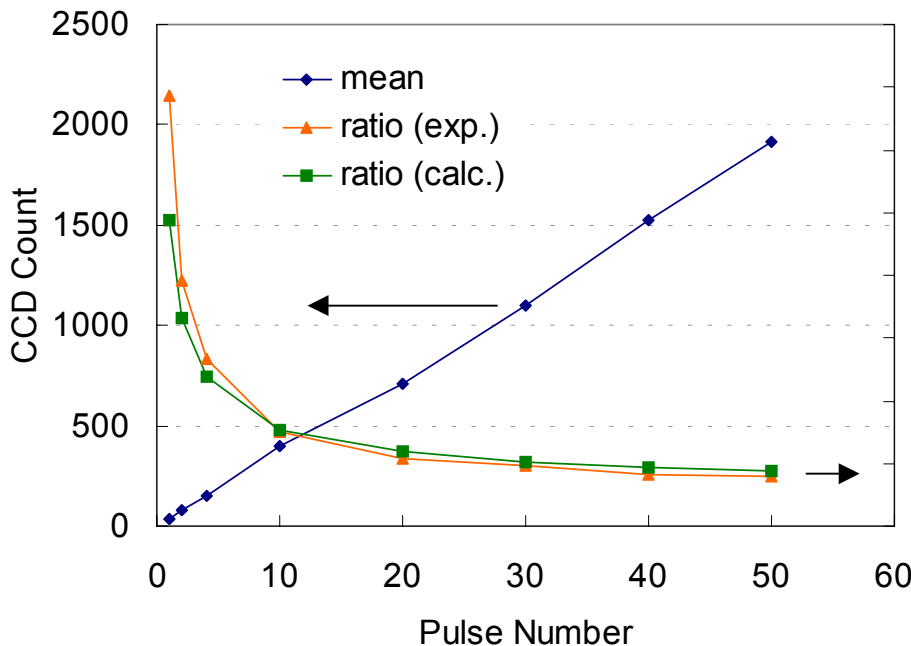
→ Roughness fluctuation smaller than original prediction of 9% by extreme fractal model due to the aberration of optics and possibly local correlation of roughness

Random = shot noise (+ readout noise) Correlation = roughness fluctuation (+ pixel sensitivity)



Impact of signal confinement degradation is relaxed by simultaneous smoothing of pixel-to-pixel fluctuation of background.

Pulse No. dependence of noise



$$\sigma_T^2 = \left(\frac{\sqrt{n_p} \cdot Q_{ED}}{n_p \cdot Q_{ED}} \cdot \alpha \right)^2 + \left(\frac{\varepsilon_R}{n_p \cdot Q_{ED}} \right)^2 + \left(\frac{\sigma_I}{\sqrt{N}} \right)^2 + (\sigma_B \cdot \beta)^2 + \sigma_p^2$$

σ_T : total fluctuation (%)

n_p : detected photon # per pixel

Q_{ED} : quantum yield of electron per detected photon

α : smoothing factor by spreading to multiple pixels

ε_R : readout noise of CCD

σ_I : random component of illumination uniformity

N : pulse number of EUV illumination

σ_B : pixel - to - pixel fluctuation of roughness

β : smoothing factor by aberration of optics

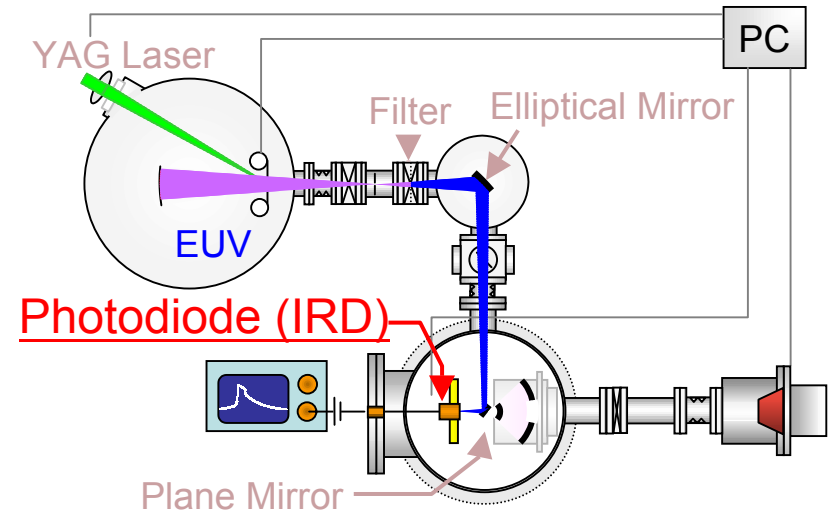
σ_p : pixel sensitivity variation

Noise almost saturates at ~ 50 pulses

-> 100 pulses appropriate for 1 image with 1/2 illumination intensity area coverage

Throughput Estimate

- Light source power
 - EUV pulse energy = 3.6×10^{-7} J
 - Images taken with 100 pulses
 - Required power = ~ 2 mW
 - @illumination for 1H TPT
 - Affordability issue, not a technical challenge
- CCD data transfer
 - 1M pixel/s (current) -> 12hrs
 - 10M pixel/s (planned) -> 75min



2 hrs per mask blank
is well within reach

Summary

- MIRAI successfully demonstrated actinic multilayer defect detection:
 - using LPP light source and dark-field imaging
 - close to “minimum critical” phase defects
 - without any false defect detection
- Throughput estimate suggests 2 hrs per mask blank is feasible
- Detailed signal characterization ongoing for prototype tool design
 - SBR a good metric to predict defect size and to reduce tool cost
 - Real-time screening algorithm developed for natural defect detection, enabling to accommodate inexpensive imaging optics
 - Two natural defects detected w/o false defect
 - 1.5nm-high “sub-critical” defect also detected w/ statistical estimate of ~20 false defect counts
 - Higher magnification will be necessary to minimize false defect

Acknowledgments

- We would like to acknowledge :
 - T. Kinoshita, T. Shoki, K. Yamashiro, O. Nagarekawa and Y. Takehana of HOYA Corporation for their fabrication of the programmed defect mask blank.
- This work was performed as part of a Ministry of Economy, Trade and Industry (METI) Project of Japan under contract with the New Energy and Industrial Technology Development Organization (NEDO).

The logo for HOYA Corporation, featuring the word "HOYA" in a bold, blue, sans-serif font.The logo for the New Energy and Industrial Technology Development Organization (NEDO), featuring a stylized blue and red circular graphic to the left of the word "NEDO" in a blue, sans-serif font.